Article

Facile Synthesis, Characterization, Anti-Microbial and Anti-Oxidant Properties of Alkylamine Functionalized Dumb-Bell Shaped Copper-Silver Nanostructures

Koduru Mallikarjuna [1,2], Amal M. Al-Mohaimeed [3] , Dunia A. Al-Farraj[4], Lebaka Veeranjaneya Reddy [5,*] , Minnam Reddy Vasudeva Reddy [6,*] and Arifullah Mohammed [7,8,*]

[1] Department for Management of Science and Technology Development, Ton Duc Thang University, Ho Chi Minh City 758307, Vietnam; koduru.mallikarjuna@tdtu.edu.vn

[2] Faculty of Applied Sciences, Ton Duc Thang University, Ho Chi Minh City 758307, Vietnam

[3] Department of Chemistry, College of Science, King Saud University, P.O. Box 22452, Riyadh 11495, Saudi Arabia; muhemeed@ksu.edu.sa

[4] Department of Botany and Microbiology, College of Science, King Saud University, P.O. Box 22452, Riyadh 11495, Saudi Arabia; dfarraj@ksu.edu.sa

[5] Department of Microbiology, Yogi Vemana University, Kadapa, Andhra Pradesh 516005, India

[6] School of Chemical Engineering, Yeungnam University, 280 Daehak-ro, Gyeongsan-si, Gyeongsangbuk-do 38541, Korea

[7] Faculty of Agro-based Industry, Jeli Campus, Universiti Malaysia Kelantan, Jeli 17600, Kelantan, Malaysia

[8] Institute of Food Security and Sustainable Agriculture, Universiti Malaysia Kelantan, Jeli 17600, Kelantan, Malaysia

* Correspondence: lvereddy@gmail.com (L.V.R.); drmvasudr9@gmail.com (M.R.V.R.); aurifullah@umk.edu.my (A.M.)

check for updates

Abstract: Admirable studies have been established on the utilization of ligand-materials as bimetallic nanoparticles in the field of nanoscience and biotechnology. UV-Vis, XRD, HR-TEM, STEM-HAADF, EDS, FTIR, and DPPH analyses characterized the optical, structural, compositional morphological, and antioxidant properties of synthesized Cu-Ag nanostructures. The spectrum of UV-Vis exhibited absorption bands at 590 and 413 nm, which reflects the surface plasmon resonance of copper-silver nanostructures. Herein, our exploration of alkylamine stabilized copper/silver nanostructures while using hexadecylamine as capping material and their primary biomedical investigation on antimicrobial and antioxidant studies is reported. Cu-Ag bimetallic nanostructures were more effective against gram-negative bacteria *E. coli* and *Klebsiella* when compared to gram-positive bacteria. The antioxidant activity of Cu-Ag nanoparticles was comparable with Ascorbic acid.

Keywords: Cu-Ag bimetallic-nanostructures; one-pot synthesis; antimicrobial; Antioxidant; DPPH free radical scavenging activity

1. Introduction

Metal nanoparticles (NPs) have enormous and admirable important applications for antimicrobials, optics, biotechnology, medicine, catalysis, microelectronics, and energy conversion, with various sizes, shapes, and composition [1]. One of the most common elements in essential biochemical pathways is copper (Cu), which is a transition metal. There have been several biologically important molecules that exhibit transfer processes, such as oxygen transfer and metal transition in their active sites.

Therefore, the more biocompatible of Cu nanoparticles (NPs) eradicate the toxicity probability, which is the main drawback of other metal NPs with medicinal value. Therefore, biosynthetic metal NPs with a variety of therapeutic potentials have recently become increasingly important. Besides, silver (Ag) is another benign and active bactericidal metal as Ag is less toxic to animal cells and very toxic to bacteria. Currently, Ag NPs are prepared by various synthesis procedures [2]. Ag NPs have antioxidant, anticancer, antiviral, anti-inflammatory, and antimicrobial properties. Furthermore, Ag NPs are used for coating or embedding for medical purposes. Moreover, to the medical applications, Ag NPs are also used in food-technology, fashion technology, paints, cosmetics, electronics, and other technologies [3]. Recent studies on bimetallic nanostructures have shown that metal-based nanomaterials can be promising catalysts by reducing material cost and improving the performance after proper moderation of their surface, composition, and nanoscale structure [4,5]. The two metal ions that are placed in the single nanostructures give the synergistic interface perspective that results in better electrical, physical, chemical properties, and biological properties leading to medical applications. Nanostructures can improve the active surface and initial electrical, optical, and chemical properties of the material [6]. In recent years, several nanocatalysts have been developed, such as noble metal catalysts Au, Pt, Ag, Pd, and Cu, for hydrogenating aromatic compounds to amino compounds [7–11]. The bimetallic alloy nanostructures have received more significant consideration due to their synergetic effects on optoelectronic and medical devices in addition to the applications of sensors, catalytic, and antioxidant in several fields. Its enormity comes from its exclusive properties, which are very different from the properties of individual metal nanoparticles [12–15]. Even though the alloy bimetallic nanomaterials, such as Pd/Cu, Pd/Ni, Au/Cu, Au/Ag, Cu/Ni, and Pd/Pt [16–18], have been reported. Recently, reports on Cu-Ag bimetallic nanoparticles have been limitedly reported. Subsequently, it is difficult to produce their alloys, because the lattice constants of Ag (0.409 nm) and Cu (0.361 nm) are different [19]. Methods have been established due to the variety and importance of these applications, such as wet, hydrothermal, microwave, and laser chemical ablation to produce nanostructure alloyed Cu-Ag [20,21]. To succeed in the above problems, a stable silver and copper catalyst is proposed, which contains a method of synthesizing bimetallic alloy nanostructures, in which silver will help to alleviate the copper oxidation. Besides, the activity can be controlled by changing the Ag and Cu ratio.

The design and development of new and advanced antibacterial agents is a very important research area due to the occurrence of novel strains of bacteria, fungi, and viruses. Additionally, many microbes acquiring resistance towards old/already present antimicrobial agents. In present situations, nanotechnology can provide the best formulations using noble metals as mono, bi, and composites form. Silver nanoparticles alone were used as antimicrobial agents against several infectious microbes and in wastewater treatment by many investigators and established its mechanism of action. Recently, very few studies were conducted on the bimetallic nanoparticle effect on microbial growth and inhibition [22,23]. Cu-Ag and other bimetallic nanoparticles were reported with enhanced activities when compared to their monometallic nanoparticle for catalytic applications [19,24]. Therefore, in this study, the copper-silver bimetallic nanostructure with dumb-bell shapes was developed while using a one-pot green synthesis method. In this synthetic process, water is used as a solvent and HDA is used as a surfactant. This simple method is useful for the fabrication of other bimetallic nanostructures at low-temperature. Moreover, the advantage of the prepared Cu-Ag nanostructures in primary medicinal applications was studied through the preliminary studies, like microbial inhibition of gram-negative and gram-positive bacterial strains, and their antioxidant properties evaluated.

2. Experimental Details

$CuCl_2 \cdot 2H_2O$, $AgNO_3$, and dextrose were acquired from Sigma–Aldrich (St. Louis, MO, USA), hexadecylamine purchased from TCI chemicals (Chuo-ku, Tokyo, Japan). In the preparation Cu-Ag dumbbell-shaped nanostructures, equal wt% of copper and silver precursors (25 mg: 25 mg; 50:50 wt%) were added to the 20 mL DI water to a glass vial (20 mL) and add 280 mg of hexadecylamine, then stir

the mixture at 35 °C for 30 min. After the 100 mg of dextrose to the mixture keep stirring for one more hour, the glass vial sealed with paraffin tape kept in the oven apply the heating 102 °C for six hours. Subsequently, the reaction vial cooled to room temperature and the compound was cleaned with IPA (isopropanol) several times.

Several analytical techniques characterized the structural and morphological properties. The optical absorption properties of Cu-Ag nanostructures were analyzed through the Thermo Scientific Genesys 10S spectrophotometer. The signature of crystallinity was obtained through the PANalytical X'pert Pro X-ray diffractometer coupled with CuKα radiation (0.154 nm). The morphological features size shape distribution and their elemental composition of the Cu-Ag nanostructure studied through the FEI Tecnai G2 F20 transmission electron microscopy that was equipped with an EDS analyzer. The functionalized modes of molecules are studied through the Thermo Scientific FTIR spectrophotometer.

2.1. Antimicrobial Activities

The antimicrobial activity of the synthesized Cu and Cu-Ag NPs was determined while using Gram-negative (*E. Coli* and *Klebsiella pneumonia*) and Gram-positive (*Bacillus sublists* and *Staphylococcus aureus*) bacteria. The microbial cultures were procured from MTCC, Chandigarh, India. The disc diffusion method was used in order to evaluate the antimicrobial potential of Cu and Cu-Ag NPs. 100 μL of overnight bacterial cultures were spread with sterile glass rod on prepared agar in Petri plates. 10 μL of 0.1 mg/mL Cu-Ag NPs were dissolved in DMSO and utilized to test the antimicrobial potential. The inhibition zone diameter (mm) was measured using Vernier calipers after incubating the bacteria for 12 h at 37 °C. The minimum inhibition concentration of the prepared nanoparticles was determined with broth by the usual twofold serial dilution method [25]. The minimum inhibition concentration (MIC) was defined as the lowest concentration of prepared NPs that inhibited the visible microbial growth after 16 h of incubation at 37 °C. The minimum bactericidal concentration (MBC), as the lowest concentration of prepared NPs that kills 99.9% of the bacteria, was also determined from the broth culture studies. MBC (lowest concentration causing bactericidal effect) was calculated as per Avadi et al. [26].

2.2. Antioxidant Activity Studies

The antioxidant activity (AA%) of Cu and Cu-Ag NPs was evaluated through the DPPH free radical scavenging capacity. The reaction mixture was comprised of 0.5 mL of Cu and Cu-Ag NPs (10–200 ug/mL), 3 mL of absolute ethanol, and 0.3 mL of DPPH solution (prepared by dissolving 0.5 mM in ethanol). The reaction between DPPH and hydrogen donating antioxidant compound resulted in the reduction of DPPH and it led to the color change from deep violet to light yellow. The absorbance (Abs) of the resulting product was read at 517 nm after 30 min. of dark incubation. The blank contains ethanol (3.3 mL) and a sample (0.5 mL). The control comprises ethanol (3.5 mL) and DPPH radical solution (0.3 mL). Finally, the DPPH free radical scavenging activity of Cu-Ag NPs was calculated from the equation below.

$$\%I = \frac{A_{blank} - A_{sample}}{A_{blank}} \times 100 \tag{1}$$

where $\%I$ = percentage inhibition, A_{blank} = absorbance of the control reaction, and A_{sample} = absorbance of the test compound.

3. Results and Discussion

The characterization of Cu-Ag bimetallic NPs was carried out while using UV-Vis spectroscopy. Figure 1 shows the absorbance spectra of copper-silver bimetallic nanostructures. The spectrum shows that the absorption band is shown at 413 nm and 590 nm. Ag NPs exhibit an absorption edge around 400–500 nm, and the Cu NPs exhibit an absorption edge around 500–600 nm, because surface plasmon

resonance shows the formation of Cu and Ag NP spectral characteristics. Due to the resonance effect of surface plasmon, noble-metal nanostructures possess collective oscillation of valance electrons and absorb the visible light region [27]. The blue shift in absorbance spectra is expected to the Cu NPs and redshift is expected to the Ag NPs. We found that the obtained results are in good agreement with the previous reports for Cu: Ag ratio [28–30]. The location of the precise metal NPs plasmon absorption band determines the shape and size of the NPs. From the above results, the coexistence of Cu and Ag indicates the formation of the bimetallic compound. For further confirmation, XRD, HR-TEM, and EDX elemental and mapping analysis were performed.
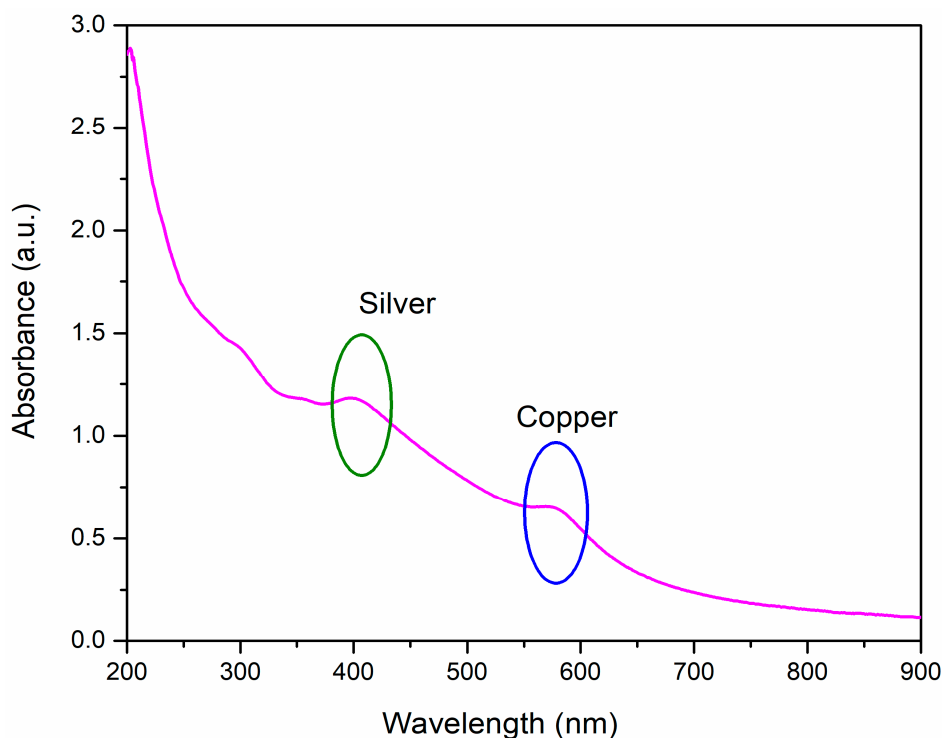

Figure 1. UV-Vis spectra of copper-silver bimetallic nanostructures.

The XRD pattern of copper-silver bimetallic NPs was recorded in the range of $2\theta = 30$–$80°$, as shown in Figure 2. The crystalline nature of the XRD peaks and possible peaks of the bimetallic copper-silver NPs are consistent with previous reports [31]. The diffraction peak positions of Ag NPs were observed at 38.2°, 44.2°, 64.3°, and 77.4° corresponding to the planes of (111), (200), (220), and (311) face-centered cubic (FCC) lattices of silver and the diffraction peak positions of Cu NPs were observed at 43.2° and 50.4° correspond to the planes of (111) and (200), and FCC lattices, respectively. The diffraction pattern of Cu-Ag NPs showed two strong (111) reflections peaks for Cu and Ag. The broadness in the peaks indicates that the Cu-Ag bimetallic is formed by the nanocrystals. The obtained results of the XRD pattern were good agreement with the Joint Committee Powder Diffraction Standards of (JCPDS) 00-04-0783 (Ag) and 00-70-3039 (Cu) diffraction data. The formation of Cu-Ag bimetallic NPs with Cu: Ag metal nanoparticles was confirmed by the XRD studies, as evidenced by the EDS analysis. Therefore, a mixture of Ag and Cu peaks were observed and no prominent XRD peaks have appeared in the possible phases of the Cu-Ag NPs. When the size of the crystallites is less than 50 nm, there is considerable broadening in the X-ray diffraction line. The particle size was estimated by the Scherrer formula to the line width of the high intense XRD peak,

$$D = \frac{k\lambda}{\beta cos\theta} \tag{2}$$

where D = average crystallite size, k = shape factor (0.94), β = angular width at FWHM, θ = Bragg angle, and λ = X-ray wavelength. The calculated crystallite size of the nanostructure was 37 nm; it matched with the TEM results well.
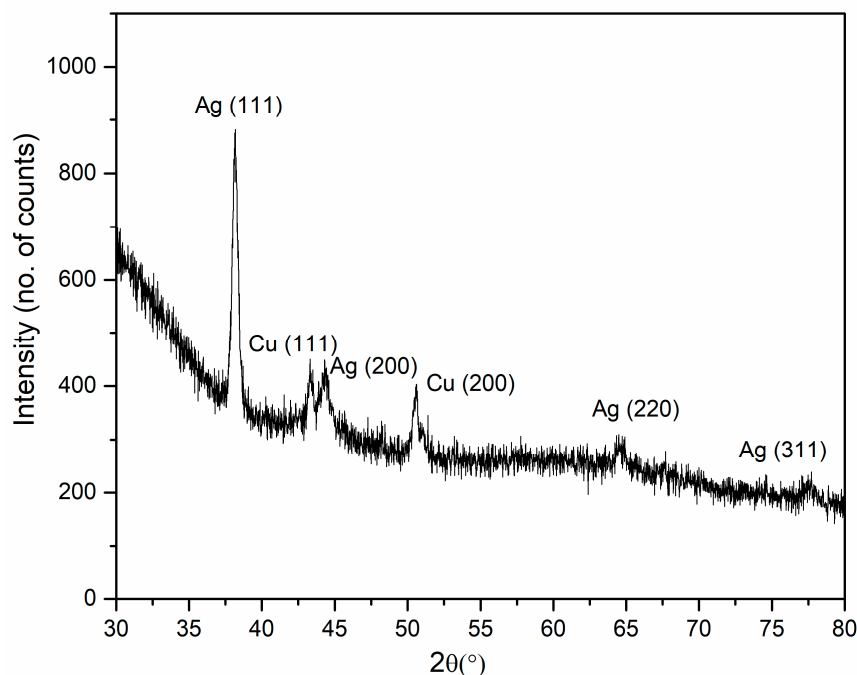

Figure 2. XRD spectrum of copper-silver bimetallic nanostructures.

The HR-TEM is the simplest and most reliable way to quantify the size of the metal NPs. It can provide the information on size and shape, but it also provides the information on the crystal structure of NPs. When energy dispersive X-ray microanalysis is used with the combination of TEM, localized basic information can be obtained. Figure 3 shows the different magnified images of HR-TEM of bimetallic nanostructures of copper-silver. From the HR-TEM images of the copper-silver bimetallic nanostructures that the image is dumb-bell shaped and the average particle size is 30–45 nm in range. The dark contrast suggested that the Ag crystals have a larger mass thickness, and light contrast indicates Cu metals. Interestingly, each particle has two distinct regions with different contrasts. Moreover, this can be observed in the HR-TEM image (Figure 3b) and Cu-Ag nanostructures evidently that are enclosed with a protecting HDA layer with a thickness of 2 ± 1 nm. Furthermore, the lattice fringes of Cu and Ag parts were observed and represented in Figure 3c, with the interplanar distance of 0.24 nm for Ag(111) and 0.21 nm represents Cu(111). In addition to that, the crystalline planes of the prepared Cu-Ag nanostructures studied through the SAED pattern (Figure 3d), which suggests the highly crystalline nature. The obtained results from HR-TEM and XRD are good consistency with the particle size. The minimum and optimal dumb-bell shape particle size dispersion of Cu-Ag NPs leads to the more active sites and large surface regions and responsible for its effective antioxidant property as well as antibacterial and electrocatalytic applications [9].

To confirm the composition and distribution of NPs, EDX analysis is applied to the spectra and elemental mapping. Figure 4 shows STEM-HAADF image, elemental mapping, and EDX spectrum images of copper-silver bimetallic nanostructures. Studies on size, shape, and morphology of the Cu-Ag nanostructures were carried out by the HR-TEM (Figure 4) and high-angle annular dark-field scanning transmission electron microscopy (HAADF-STEM), which is shown in Figure 4a. The elemental mapping profile of synthesized copper-silver bimetallic NPs shows the presence of copper (Figure 4b) and silver (Figure 4c). From the elemental mapping (Figure 4b,c), it is indicated that the Cu and Ag are mostly separately distributed. The presence of Cu and Ag elements was observed (Figure 4d) and no other impurities were founded, as observed from the EDX spectrum.
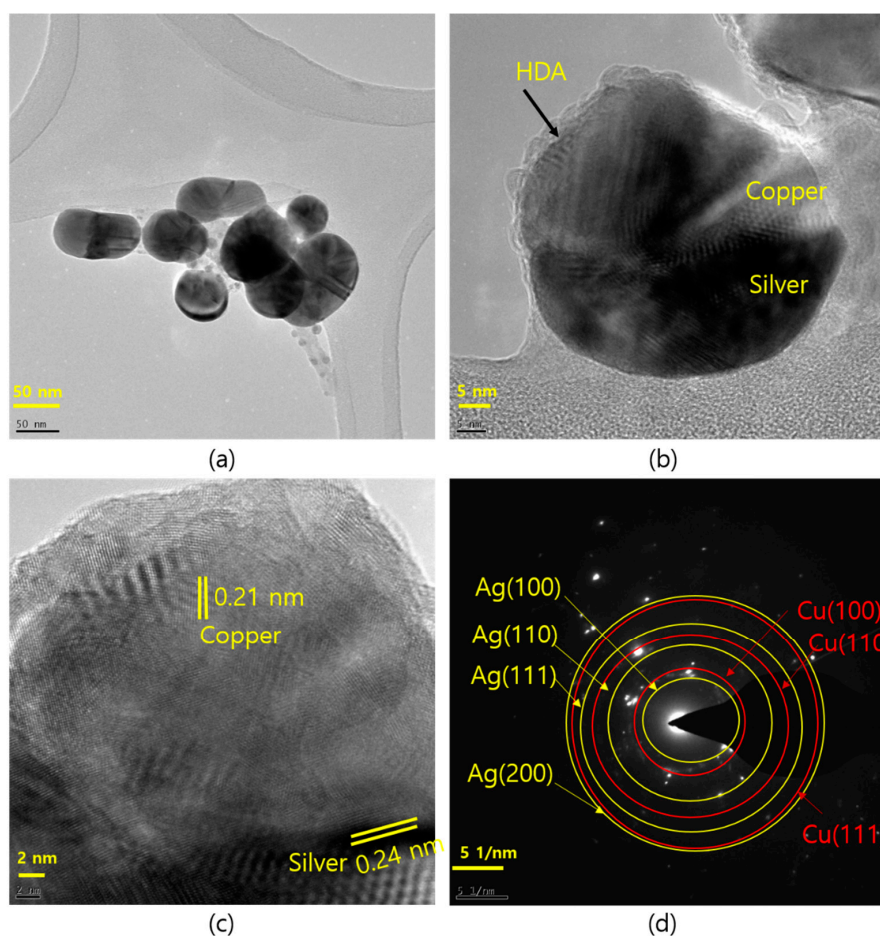
Figure 3. Different magnification HR-TEM images of copper-silver bimetallic nanostructures: (**a**) 100 nm; (**b**) representing the silver and copper nanoparticles with hexadecylamine (had) layer; (**c**) lattice fringes of Cu-Ag nanoparticle; and, (**d**) SAED pattern of Cu-Ag nanoparticles.
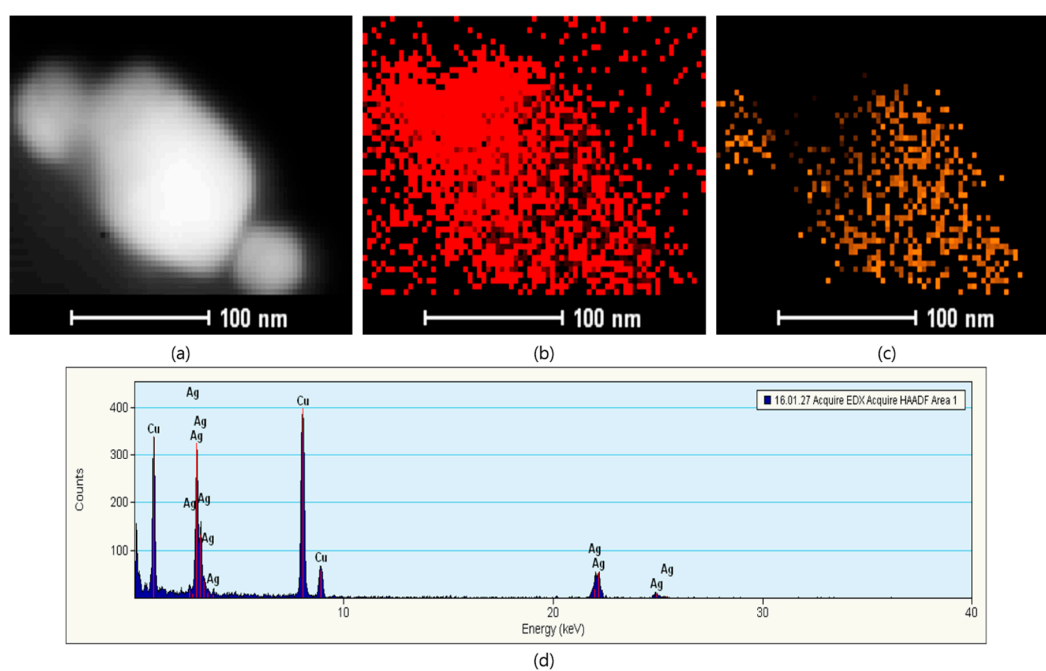

Figure 4. STEM-HAADF, elemental mapping, and EDX spectrum of copper-silver bimetallic nanostructures: (**a**) STEM-HAADF image; (**b**) copper; (**c**) silver; and, (**d**) EDX spectrum.

Generally, the qualitative and quantitative analysis of the material's homogeneity was studied by the Fourier transform infrared (FT-IR). FTIR spectroscopy is a significant technique for studying the role of hexadecylamine (HDA) in the synthesis of Cu-Ag bimetallic nanostructures and their surface environments. It can be seen from Figure 5 that the N-H stretching produces symmetrical (3329 cm^{-1}), asymmetrical (3251 and 3153 cm^{-1}) stretching vibration peaks, and the vibration modes at 2918 and 2854 cm^{-1} are correspondingly assigned to the C-H stretching terminal modes of the CH_3 and CH_2 group alkyl chains of HDA [32]. The peak that was obtained at 1607 cm^{-1} is related to the vibration modes of N-H bending and modes at 1464 and 1362 cm^{-1} are related to the C-H bending vibration modes of the CH_3 and CH_2, respectively [33]. For the bimetallic nanostructures of Cu-Ag, there is a lower wavenumber of about 45 cm^{-1} due to the binding of the amine group that was adsorbed on the HDA surface of the bimetallic nanostructures of Cu-Ag, indicating that the organic residue is part of the fabrication of bimetallic nanostructures [34].
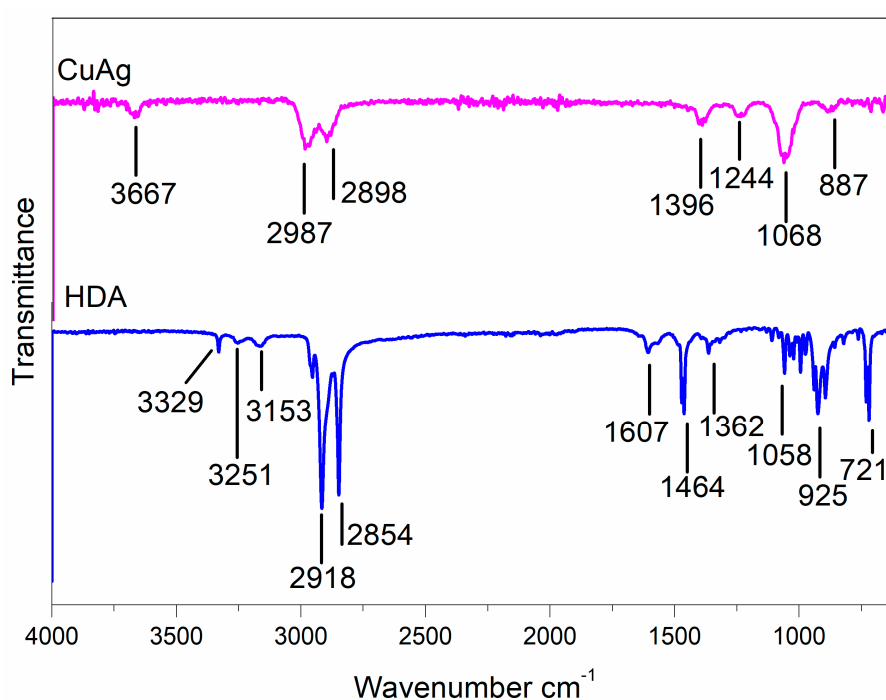

Figure 5. FTIR spectra of copper-silver bimetallic nanostructures and hexadecylamine.

The antimicrobial property of Copper and synthesized copper and silver nanostructures was evaluated through the zone inhibition test. The prepared nanomaterials were screened for their antimicrobial property on both Gram-positive and Gram-negative microorganisms. For this, we have selected two Gram-positive (*Bacillus subtilis*, *Staphylococcus aureus*) and two Gram-negative (*E. coli*, *Klebsiella pneumonia*) microorganisms. Cu-Ag nanostructures showed higher inhibition activity for both Gram-positive and Gram-negative microorganisms when compared to Cu alone. Minimum inhibition concentration (MIC) and minimum bactericidal concentration (MBC) were also calculated for prepared Cu-Ag nanostructures. Table 1 and Figure 6 provide the zone of inhibition measurements, MIC, and MBC values. From the table, one can suggest that Cu-Ag nanostructures at 100 µg/mL have better antimicrobial activity when compared to 50 µg/mL NPs. Cu NPs and Ag NPs each alone have antimicrobial activity. Soluble copper that entered into bacteria is toxic; hence, it is antimicrobial. Particulate copper had a low association with the bacterial membrane, but the soluble one easily enters and accumulates high intra-bacterial levels and, hence, the solubility is very important for copper antimicrobial activity [35]. In the case of Cu-Ag bimetallic nanostructures, the inhibition zone increases with increasing Ag concentrations, which again supports the efficiency of Ag nanoparticles.

The figure indicates that Cu-Ag bimetallic nanostructures were more effective against gram-negative bacteria *E. coli* and *Klebsiella*, due to the difference in cell wall structure between gram-negative and gram-positive microorganisms. From the bimetallic nanostructures, silver and copper ions released and attach to the negatively charged bacterial cell wall and disrupt it, in this manner causing protein denaturation and cell death [36]. MIC and MBC of Cu-Ag nanoparticles against the screened four bacterial cultures indicated that the metallic nanoparticles showed very good antibacterial activity against bacteria, even at concentrations as low as 23 µg/mL. Therefore, it could be concluded that silver and copper ions could benefit long duration activity and preserve sustained microbial inhibition.

Table 1. The comparison of antibacterial studies of prepared nanostructures with gram-negative and gram-positive bacterial strains.

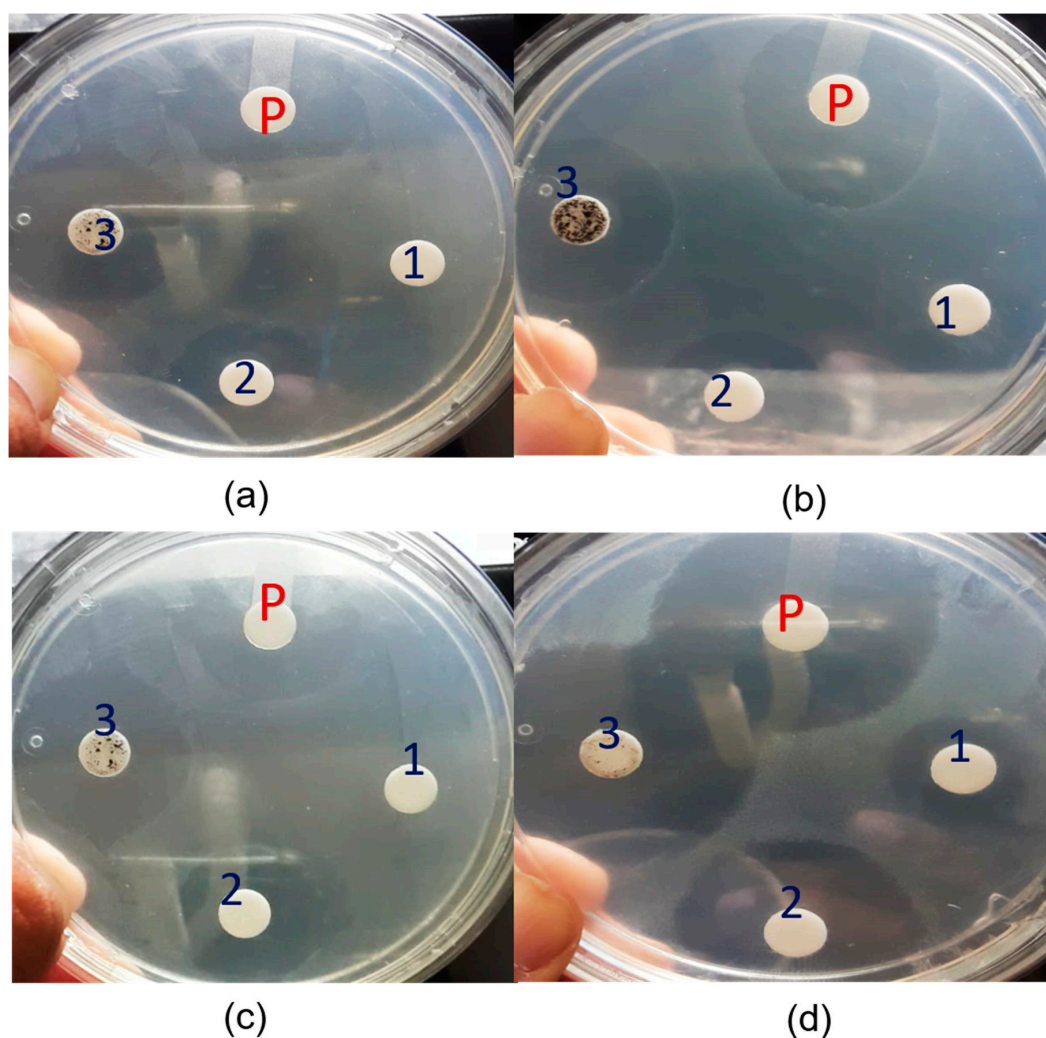| Activity Name	Zone of Inhibition (mm)			MIC (µg/mL)	MBC (µg/mL)
	P	Cu-Ag (50 µg/mL)	Cu-Ag (100 µg/mL)		
E. coli	23	20	28	23	85
K. pneumoniae	15	15	20	36	97
B. subtilis	18	14	20	38	132
S. aureus	20	12	16	40	148

Figure 6. Photographs of Antimicrobial activity of Cu-Ag NPs against different bacteria: (**a**) *Bacillus*, (**b**) *Staphylococcus*, (**c**) *Klebsiella*, and (**d**) *E. coli* (P–Penicillin, 1-DMSO, 2- Cu (50 ug), 3- Cu-Ag (100 ug).

　　　Antimicrobial activity of Cu-Ag NPs is mainly because of the silver or copper ions released from the Cu-Ag NPs may attach to the negatively charged bacterial cell wall and damage it and lead to intracellular entry and cause protein and genetic material denaturation and, finally, cause the cell death [37].

Antioxidant Activity of Cu-Ag Nanostructures

　　　DPPH is a stable free radical scavenger that exhibits characteristic absorption at 517 nm and 700 nm wavelength. After reduction, the color becomes different from violet to yellow [38]. The antioxidant property was measured according to Ferrari et al. [39]. Figure 7a displays the DPPH free radical scavenging activity of Cu-Ag NPs. DPPH has been widely used as a stable free to assess reducing substances and their useful reagent to study the free radical scavenging activity. The antioxidant reacts with DPPH and converts it to 1, 1- diphenyl-2-picryl hydrazine with de-colorization. Cu-Ag NPs exhibited the higher free radical scavenging ability than Cu NPs (Figure 7b), due to the effective oxidation of Cu-Ag NPs. The Cu-Ag NPs satisfied the DPPH activity by providing copper electrons. Finally, the DPPH free radical scavenging activity of Cu-Ag NPs was calculated from the equation given below in the Methods section [40].
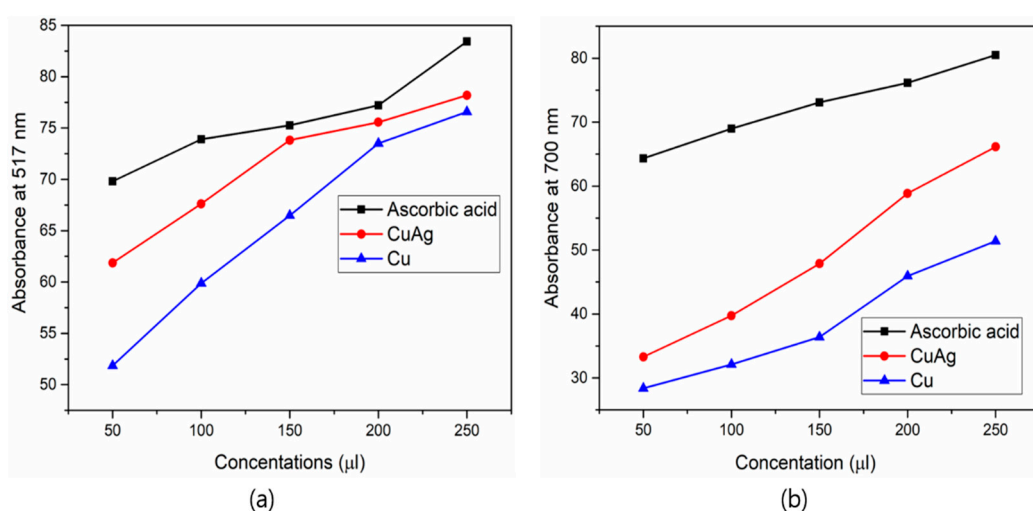

Figure 7. (**a**). Antioxidant activity Cu-Ag NPs by DPPH assay at a characteristic absorption of 517 nm (**b**) antioxidant activity Cu-Ag NPs by DPPH assay at a characteristic absorption of 700 nm.

4. Conclusions

　　　In the present work, the Cu-Ag NPs were synthesized by the easy, cost-effective, and eco-friendly one-pot green synthesis process. The synthesized Cu-Ag bimetallic NPs were stable and reproducible. The characterizations, such as UV–vis, FT-IR, XRD, EDS, and HR-TEM analysis, showed the formation of Cu-Ag bimetallic NPs. The synthesized copper-silver nanoparticles were in a dumb-bell shape with the size range of 30–45 nm. The Cu-Ag NPs had excellent antioxidant activity and the antioxidant activity was performed using DPPH assay. The dumbbell-shaped Cu-Ag bimetallic nanostructures were more effective against gram-negative bacteria *E. coli* and *Klebsiella* than gram-positive microorganisms. The Cu-Ag bimetallic NPs can be used as a very good antioxidant medicine in the future.

Author Contributions: K.M. performed the experimental work and written the original MS; A.M.A.-M. provided resources A.-F.A. provided funding; L.V.R. conceptualization wrote the manuscript; M.R.V.R. revised and edited the manuscript, and A.M. analyzed the data and supervised the work. All authors have read and agreed to the published version of the manuscript.

Conflicts of Interest: The authors declare no conflict of interest.

References

1. Cao, S.; Tao, F.; Tang, Y.; Li, Y.; Yu, J. Size-and shape-dependent catalytic performances of oxidation and reduction reactions on nanocatalysts. *Chem. Soc. Rev.* **2016**, *45*, 4747–4785. [CrossRef] [PubMed]

2. Zhang, X.-F.; Liu, Z.-G.; Shen, W.; Gurunathan, S. Silver nanoparticles: Synthesis, characterization, properties, applications, and therapeutic approaches. *Int. J. Mol. Sci.* **2016**, *17*, 1534. [CrossRef] [PubMed]

3. Beyene, H.D.; Werkneh, A.A.; Bezabh, H.K.; Ambaye, T.G. Synthesis paradigm and applications of silver nanoparticles (AgNPs), a review. *Sustain. Mater. Technol.* **2017**, *13*, 18–23. [CrossRef]

4. Gilbertson, L.M.; Zimmerman, J.B.; Plata, D.L.; Hutchison, J.E.; Anastas, P.T. Designing nanomaterials to maximize performance and minimize undesirable implications guided by the Principles of Green Chemistry. *Chem. Soc. Rev.* **2015**, *44*, 5758–5777. [CrossRef]

5. Rodrigues, T.S.; da Silva, A.G.M.; Camargo, P.H.C. Nanocatalysis by noble metal nanoparticles: Controlled synthesis for the optimization and understanding of activities. *J. Mater. Chem. A* **2019**, *7*, 5857–5874. [CrossRef]

6. Khan, I.; Saeed, K.; Khan, I. Nanoparticles: Properties, applications and toxicities. *Arab. J. Chem.* **2017**, *12*, 908–931. [CrossRef]

7. Anandkumar, M.; Vinothkumar, G.; Babu, K.S. Synergistic effect of gold supported on redox active cerium oxide nanoparticles for the catalytic hydrogenation of 4-nitrophenol. *New J. Chem.* **2017**, *41*, 6720–6729. [CrossRef]

8. Wu, Z.; Yang, S.; Wu, W. Shape control of inorganic nanoparticles from solution. *Nanoscale* **2016**, *8*, 1237–1259. [CrossRef]

9. Saha, S.; Pal, A.; Kundu, S.; Basu, S.; Pal, T. Photochemical green synthesis of calcium-alginate-stabilized Ag and Au nanoparticles and their catalytic application to 4-nitrophenol reduction. *Langmuir* **2010**, *26*, 2885–2893. [CrossRef]

10. Lv, J.-J.; Wang, A.-J.; Ma, X.; Xiang, R.-Y.; Chen, J.-R.; Feng, J.-J. One-pot synthesis of porous Pt–Au nanodendrites supported on reduced graphene oxide nanosheets toward catalytic reduction of 4-nitrophenol. *J. Mater. Chem. A* **2014**, *3*, 290–296. [CrossRef]

11. Xia, J.; He, G.; Zhang, L.; Sun, X.; Wang, X. Hydrogenation of nitrophenols catalyzed by carbon black-supported nickel nanoparticles under mild conditions. *Appl. Catal. B Environ.* **2016**, *180*, 408–415. [CrossRef]

12. Ferrando, R.; Jellinek, J.; Johnston, R.L. Nanoalloys: From theory to applications of alloy clusters and nanoparticles. *Chem. Rev.* **2008**, *108*, 845–910. [CrossRef] [PubMed]

13. Burda, C.; Chen, X.; Narayanan, R.; El-Sayed, M.A. Chemistry and properties of nanocrystals of different shapes. *Chem. Rev.* **2005**, *105*, 1025–1102. [CrossRef] [PubMed]

14. Rodriguez, J.A.; Goodman, D.W. The nature of the metal-metal bond in bimetallic surfaces. *Science* **1992**, *257*, 897–903. [CrossRef]

15. Francesco, I.N.; Fontaine-Vive, F.; Antoniotti, S. Synergy in the catalytic activity of bimetallic nanoparticles and new synthetic methods for the preparation of fine chemicals. *ChemCatChem* **2014**, *6*, 2784–2791. [CrossRef]

16. Fu, F.; Cheng, Z.; Lu, J. Synthesis and use of bimetals and bimetal oxides in contaminants removal from water: A review. *RSC Adv.* **2015**, *5*, 85395–85409. [CrossRef]

17. Medici, S.; Peana, M.; Nurchi, V.M.; Lachowicz, J.I.; Crisponi, G.; Zoroddu, M.A. Noble metals in medicine: Latest advances. *Coord. Chem. Rev.* **2015**, *284*, 329–350. [CrossRef]

18. Zang, W.; Li, G.; Wang, L.; Zhang, X. Catalytic hydrogenation by noble-metal nanocrystals with well-defined facets: A review. *Catal. Sci. Technol.* **2015**, *5*, 2532–2553. [CrossRef]

19. Valodkar, M.; Modi, S.; Pal, A.; Thakore, S. Synthesis and anti-bacterial activity of Cu, Ag and Cu–Ag alloy nanoparticles: A green approach. *Mater. Res. Bull.* **2011**, *46*, 384–389. [CrossRef]

20. Wu, W.; Lei, M.; Yang, S.; Zhou, L.; Liu, L.; Xiao, X.; Jiang, C.; Roy, V.A.L. A one-pot route to the synthesis of alloyed Cu/Ag bimetallic nanoparticles with different mass ratios for catalytic reduction of 4-nitrophenol. *J. Mater. Chem. A* **2015**, *3*, 3450–3455. [CrossRef]

21. Peng, X.; Pan, Q.; Rempel, G.L. Bimetallic dendrimer-encapsulated nanoparticles as catalysts: A review of the research advances. *Chem. Soc. Rev.* **2008**, *37*, 1619–1628. [CrossRef] [PubMed]

22. Yoon, K.-Y.; Hoon Byeon, J.; Park, J.-H.; Hwang, J. Susceptibility constants of *Escherichia coli* and *Bacillus subtilis* to silver and copper nanoparticles. *Sci. Total Environ.* **2007**, *373*, 572. [CrossRef]

23. Ruparelia, J.P.; Chatterjee, A.K.; Duttagupta, S.P.; Mukherji, S. Strain specificity in antimicrobial activity of silver and copper nanoparticles. *Acta Biomater.* **2008**, *4*, 707–716. [CrossRef]

24. Perdikaki, A.; Galeou, A.; Pilatos, G.; Karatasios, I.; Kanellopoulos, N.K.; Prombona, A.; Karanikolos, G.N. Ag and Cu monometallic and Ag/Cu bimetallic nanoparticle—Graphene composites with enhanced antibacterial performance. *ACS Appl. Mater. Interfaces* **2016**, *8*, 27498–27510. [CrossRef] [PubMed]

25. Cho, K.; Park, J.; Osaka, T.; Park, S. The study of antimicrobial activity and preservative effects of nanosilver ingredient. *Electrochim. Acta* **2005**, *51*, 956–960. [CrossRef]

26. Avadi, M.R.; Sadeghi, A.M.M.; Tahziba, A.; Bayati, K.; Pouladzadeh, M.; Zohuriaan, M.J. Diethylmethyl chitosan as an antimicrobial agent: Synthesis, characterization and antibacterial effects. *Eur. Polym. J.* **2014**, *40*, 1355–1361. [CrossRef]

27. Bansal, A.; Verma, S.S. Optical response of noble metal alloy. *Phys. Lett. A* **2015**, *379*, 163–169. [CrossRef]

28. Yallappa, S.; Manjanna, J.; Sindhe, M.A.; Satyanarayan, N.D.; Pramod, S.N.; Nagaraja, K. Microwave assisted rapid synthesis and biological evaluation of stable copper nanoparticles using *T. arjuna* bark extract. *Spectrochim. Acta Part A Mol. Biomol. Spectrosc.* **2013**, *110*, 108–115. [CrossRef]

29. Yallappa, S.; Manjanna, J. Biological evaluation of silver nanoparticles obtained from *T. arjuna* bark extract as both reducing and capping agent. *J. Clust. Sci.* **2014**, *25*, 1449–1462. [CrossRef]

30. Banik, M.; Patra, M.; Dutta, D.; Mukherjee, R.; Basu, T. A simple robust method of synthesis of copper–silver core–shell nano-particle: Evaluation of its structural and chemical properties with anticancer potency. *Nanotechnology* **2018**, *29*, 325102. [CrossRef]

31. Bar, H.; Bhui, D.K.; Sahoo, G.P.; Sarkar, P.; Pyne, S.; Misra, A. Green synthesis of silver nanoparticles using seed extract of *Jatropha curcas*. *Colloids Surf. A Physicochem. Eng. Asp.* **2009**, *348*, 212–216. [CrossRef]

32. Nath, S.; Praharaj, S.; Panigrahi, S.; Kundu, S.; Ghosh, S.K.; Basu, S.; Pal, T. Hexadecylamine capped silver organosol: A substrate for surface enhanced Raman scattering. *Colloids Surf. A Physicochem. Eng. Asp.* **2006**, *274*, 145–149. [CrossRef]

33. Hou, X.; Zhang, X.; Fang, Y.; Chen, S.; Li, N.; Zhou, Q. 1-Hexadecylamine as both reducing agent and stabilizer to synthesize Au and Ag nanoparticles and their SERS application. *J. Nanopart. Res.* **2011**, *13*, 1929–1936. [CrossRef]

34. Mallikarjuna, K.; Kim, H. Synthesis of shape and size-dependent CuAg bimetallic dumbbell structures for organic pollutant hydrogenation. *Physica. E Low-Dimens. Syst. Nanostruct.* **2018**, *102*, 44–49. [CrossRef]

35. Bastos, C.A.P.; Faria, N.; Wills, J.; Malmberg, P.; Scheers, N.; Rees, P.; Powell, J.J. Copper nanoparticles have negligible direct antibacterial impact. *NanoImpact* **2020**, *17*, 100192. [CrossRef]

36. Lin, Y.S.E.; Vidic, R.D.; Stout, J.E.; McCartney, C.A.; Yu, V.L. Inactivation of *Mycobacterium avium* by copper and silver ions. *Water Res.* **1998**, *32*, 1997–2000. [CrossRef]

37. Lin, H.-Y.; Chou, C.-C. Antioxidative activities of water-soluble disaccharide chitosan derivatives. *Food Res. Int.* **2004**, *37*, 883–889. [CrossRef]

38. Srihasam, S.; Thyagarajan, K.; Korivi, M.; Lebaka, V.R.; Mallem, S.P.R. Phytogenic generation of NiO nanoparticles using stevia leaf extract and evaluation of their in-vitro antioxidant and antimicrobial properties. *Biomolecules* **2020**, *10*, 89. [CrossRef] [PubMed]

39. Ferrari, E.; Asti, M.; Benassi, R.; Pignedoli, F.; Saladini, M. Metal binding ability of curcumin derivatives: A theoretical vs. experimental approach. *Dalton Trans.* **2013**, *42*, 5304–5313. [CrossRef]

40. Govindappa, M.; Hemashekhar, B.; Arthikala, M.-K.; Ravishankar Rai, V.; Ramachandra, Y.L. Characterization, antibacterial, antioxidant, antidiabetic, anti-inflammatory and antityrosinase activity of green synthesized silver nanoparticles using *Calophyllum tomentosum* leaves extract. *Results Phys.* **2018**, *9*, 400–408. [CrossRef]